A Framework for Sense and Follow Convoys for Collective Autonomous Mobility

Abraham K. Ishihara*
KBR, Moffett Field, CA, 94305

Husni Idris†
NASA, Moffett Field, CA, 94305

Min Xue‡
NASA, Moffett Field, CA, 94305

Convoys are collections of vehicles that share similar velocity profiles. In the sense-and-follow convoy construct, a vehicle can follow a member of an existing convoy resulting in convoy chaining. We prove conditions under which this can occur such that the resulting convoy chain is bounded and the velocities of all members converge to the leader velocity through locally distributed control algorithms. To assess the approach, we utilize a six degree-of-freedom rigid-body vehicle dynamics model for each agent. A dynamic inversion based control law is used to track the desired trajectory generated by the convoy algorithms. To simulate the system, we utilize Unity, a cross-platform game engine, where 3-dimensional terrain, building, and vehicle data can be visualized. Numerous simulations are presented to illustrate the concept.

I. Introduction

We are at the cusp of an aviation revolution whereby flying cyber-physical systems will disrupt and transform entire industries. Rapid advancements in new technologies spanning electric propulsion to vehicle autonomy coupled with innovative business models have given rise to a new aviation market termed Urban Air Mobility (UAM). Morgan Stanley posits a market potential of 1.5 trillion by 2040 [1].

The challenges, however, abound. High density operations may become prevalent in the urban setting motivating the need for more efficient modes of operation. Autonomy will play a central role to enable scalability of operations by removing the barrier of human-centric centralized traffic control. UAM vehicles grouped in convoys have the potential to lead to improved utilization of the airspace, reducing the workload of human airspace controllers, and thereby increasing the autonomy of the system overall. By convoy is meant a collection of vehicles that share a common velocity profile and are bounded in a sense to be made precise below in Section II. For example, a convoy of cars on a highway share a common velocity typically set by the leader of the convoy, which can result in increasing throughput. A driver in the right (slower) lane, might find it advantageous to join a faster moving convoy on the left if the velocity profile is acceptable. These decisions depend on various objective functions and vehicle performance characteristics. The dynamics of a slow moving truck might prevent it from joining a fast moving convoy on a windy road and a driver of a vehicle may not feel comfortable driving at a higher speed due to the potential of getting a speeding ticket. In current aviation processes, air traffic controllers often group flights by performance characteristics such as speed or destination to reduce their workload and increase airspace capacity. As aircraft approach their destination they are merged and compressed and once their desired spacing is achieved their speeds are matched such that they maintain their spacing as one object. In this manner controllers are able to monitor and control a larger number of aircraft that are chained together, thus increasing airspace capacity [2]. Often an aircraft is instructed by air traffic controllers to follow another aircraft on visual approach which achieves higher runway throughput. Similarly in uncontrolled airspace, pilots identify other aircraft to follow in the visual approach pattern in a distributed manner.

As the future UAM environment expects higher traffic density, centralized human-based control becomes infeasible and distributed autonomous schemes become critical. Convoys emerging and forming in a distributed manner is envisioned in this paper as a mechanism to increase scalability by enabling a small number of human operators to

*NASA Ames Research Center, Moffett Field, CA., AIAA Member
†NASA Ames Research Center, Moffett Field, CA., AIAA Associate Fellow
‡NASA Ames Research Center, Moffett Field, CA., AIAA Senior Member

supervise convoys of a large number of vehicles as one cohesive object and by enabling traffic structure to emerge when and where needed (for example to avoid weather hazards) rather than being imposed a priori through, for example, fixed corridors and procedures.

In the study of convoys, several questions naturally emerge: What is the long-term collective behavior of vehicles in a convoy? What are the sensing, control, and communication requirements? How can a vehicle determine if it is advantageous to participate? What are the objective functions to be considered when joining or leaving a convoy? How can a service mediate or facilitate convoy operations?

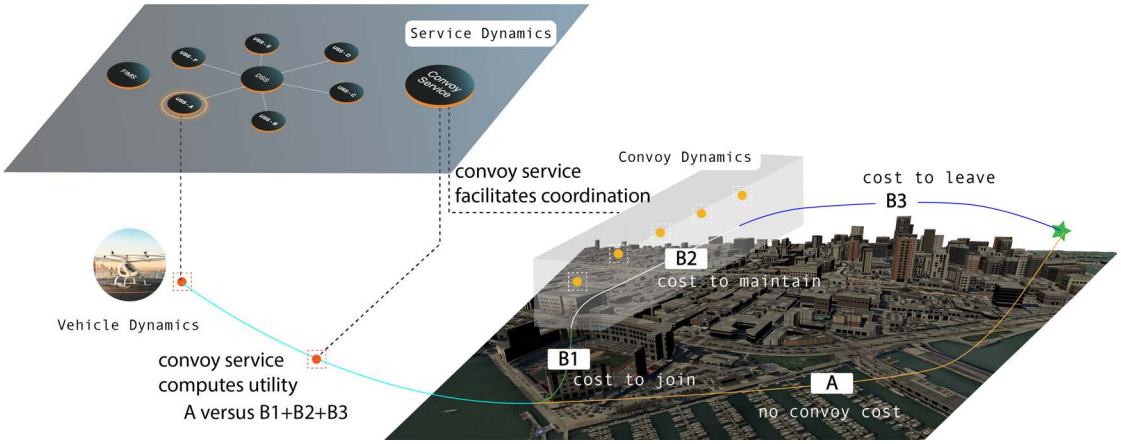

Fig. 1 Figure depicts three aspects: (1) Convoy dynamics, (2) Cost or utility function computation to join or leave a convoy, (3) Convoy service to mediate or facilitate participation in a UTM-like environment.

This paper focuses on the collective behavior of vehicles in a new construct termed 'sense and follow' convoys where chains of sub-convoys can emerge. In this framework, a single vehicle traveling to a destination along some (potentially optimized) trajectory could serve as a catalyst for the formation of a multi-chain convoy by allowing other vehicles to sense and follow it if it were deemed advantageous to do so. We envision third party services operating within a UTM (UAS Traffic Management) architecture that could facilitate policies, decision making, vehicle objective function computation, and interaction with traffic management services to enable spontaneous formation of convoys and their dissociation. These notions are depicted in Fig. 1.

The contributions of this paper are as follows: (1) we prove conditions under which a vehicle can join a particular class of convoy architectures such that it remains bounded and that the velocities of all agents converge to the leader velocity; (2) we demonstrate a Unity based platform for multi-agent simulation over the web that implements the convoy algorithms and enables evaluation of collective behavior.

Previous Work: Much of the literature in convoy formation has been driven by ground transportation system applications. Henke et al. [3, 4] investigated convoy formation in autonomous railway vehicles in order to increase track capacity and decrease overall energy consumption. Several use-cases were evaluated including joining and leaving convoys. Communication protocols were developed to facilitate communication between non-members and existing convoys. Khan et al. [5], investigated convoy formation in a highway autonomous driving setting where ad-hoc convoys can form, split, and merge mediated by V2V (Vehicle to Vehicle) communication. Vehicle interaction within a convoy evolved according to socio-potential field (attraction, repulsion), but did not include any alignment terms (terms that involve differences between agent velocity vectors). To determine whether or not a vehicle should join a given convoy, a policy involving a utility dependent on the difference between the average convoy velocity and the vehicle's desired velocity was utilized. Extending this approach to include vehicle position information in the utility function was considered in [6] where vehicles further away from a convoy incurred a higher penalty than vehicles that were closer. Central to the intra-convoy vehicle trajectory evolution explored in [5] and in other agent based systems is a class of algorithms originally proposed by Cucker and Smale [7]. A continuous time system account was analyzed in [8, 9] and constitutes the basis for the analysis presented herein.

Lastly, we mention that the term flocking or swarming is often used in the literature to describe or model collective behavior observed in biological systems or to motivate the design of guidance and control systems for unmanned vehicles operating in air, ground, underwater, or space environments. We point out a few differences. Let $x_i \in \mathbb{R}^3$ and $v_i \in \mathbb{R}^3$

denote, respectively, the position and velocity of agent $i \in [1, N]$ where N is the number of agents in the collection. A collection of agents is said to be *cohesive* if there exists a constant $b > 0$ such that $\sup_t \max_{i,j\in[1,N]} \|x_i(t) - x_j(t)\| < b$. A collection of agents is said to be *aligned* if $\lim_t \max_{i,j\in[1,N]} \|v_i(t) - v_j(t)\| = 0$.

The term flocking is meant to describe the behavior of a collection of agents characterized by velocity *alignment*, that is, the convergence of all agent velocities to a common one as defined above. The inter-agent separation distances, by virtue of *alignment*, remain constant and the diameter of the flock (considered as a set in $\mathbb{R}^3$) is finite. A consequence of flocking is, therefore, *cohesion*. On the other hand, the term swarming is meant to describe the behavior of a collection of agents characterized by *cohesion*. Alignment is not necessarily a consequence of swarming. We refer to a convoy as a flock that has a specific topological structure and implements locally distributed control and communication algorithms that give rise to emergent behavior. This will be made precise in the next section.

II. Analysis of Convoys

We are interested in a class of locally distributed algorithms that govern the dynamics of each agent. By locally is meant each agent requires information (position and velocity) of other agents that are local to it as defined by a specified metric. This paper focuses on a combination of both spatial and topological metrics. By distributed is meant each individual agent computes its dynamics given local information (as discussed previously) from other agents as opposed to it (the dynamics) being computed by a central system and then transmitted to each agent. Fig. 2 depicts the notion of local information and distributed computation.

In the following, we present a framework motivated by the work in [8–10].

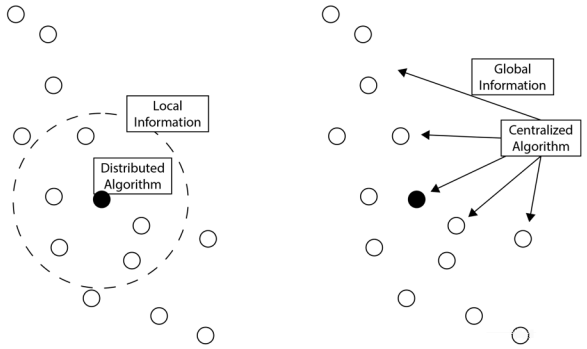

Fig. 2 Illustration of a locally distributed approach versus a globally centralized one.

Definition II.1. *An N-convoy consists of a collection of N agents, each governed by the following nonlinear ordinary differential equation:*

$$\begin{cases} \dot{x}_i = v_i \\ \dot{v}_i = \beta \sum_{j\in I_i} \beta_{ij} \left(v_j - v_i\right) + l_i \\ x_i(t_0) = x_{i0}; v_i(t_0) = v_{i0} \end{cases} \tag{1}$$

where $\beta > 0$; $\beta_{ij} : \bar{\mathbb{R}}^+ \to \bar{\mathbb{R}}^+$ represents the influence agent j has on agent i and is given by

$$\beta_{ij} = \zeta_{ij}\phi(\|x_i - x_j\|) \tag{2}$$

where

$$\zeta_{ij} = \begin{cases} 1 & \text{if } j \text{ connects to } i \\ 0 & o/w \end{cases} \tag{3}$$

and $\phi : \bar{\mathbb{R}}^+ \to [0, 1]$ is a non-increasing, non-negative function with compact support, that is, there exists a $\sigma > 0$ such that $\phi(r) = 0$ for all $r \geq \sigma$ with $\phi(0) = 1$; $l_i : \bar{\mathbb{R}}^+ \to \mathbb{R}$ represents attraction, repulsion, and leadership terms; $(x_{i0}, v_{i0}) \in E \times E$ denote the initial conditions of agent i where $E = \mathbb{R}^d$ and $d \in [1, 3]$, $i \in [1, N]$; and $I_i := [1, N] \setminus \{i\}$. The term l_i the case of a leader (discussed below), could be derived from a trajectory optimization algorithm that minimizes a cost while avoiding constraints such as a weather cell or an emergency event. In the present paper, we assume it to be zero for leaders (which implies constant velocities) and repulsive terms for followers in order to guarantee collision avoidance.

Definition II.2 (Agent Influence)**.** *Agent j is said to influence agent i at time $t \geq t_0$ if $\beta_{ij} > 0$.*

Remark 1. *ζ_{ij} is a pre-configuration term that represents the existence of a connection from agent j to agent i. ϕ represents the strength of the connection between agents, if it exists, and σ, a finite sensing or communication distance. In the case of sensing, this could represent on-board radar, or in the case of communication, Dedicated Short-Range Communications (DSRC). In both cases, and for different reasons, uncertainty, errors, time-delay, etc., can exist. We do not consider any of these aspects in this paper. By Definition II.2, agent j influences agent i if and only if agent j is connected to agent i and that connection has non-zero strength.*

Definition II.3 (Connectivity Matrix)**.**
The connectivity matrix, $G \in \mathbb{R}^{N\times N}$, whose i^{th} row and j^{th} column is given by ζ_{ij}, represents the configuration of the convoy in (1). The terms, $\delta_{ii}; i \in [1, N]$, which comprise the diagonal of G, are defined to be zero. This is interpreted to mean an agent cannot connect to itself.

Remark 2. *The connection term, ζ_{ij}, is directional; if agent j is connected to agent i, agent i may or may not be connected to agent j. Hence, matrix G is generally not symmetric.*

Definition II.4 (Connectivity Sets)**.** *The connectivity set for agent i is defined by*

$$\Gamma_i := \{j \in [1, N] : \zeta_{ij} = 1\} \tag{4}$$

The non-connectivity set for agent i is defined by

$$\Gamma_i' := \{j \in I_i : \zeta_{ij} = 0\} \tag{5}$$

Lastly, we will also want a notation to include agent i in the connectivity set. Hence, define

$$\bar{\Gamma}_i := \Gamma_i \cup \{i\} \tag{6}$$

We may write $[1, N] = \{i\} \cup \Gamma_i \cup \Gamma_i' = \bar{\Gamma}_i \cup \Gamma_i'$. The sum in (1) does not include $j = i$ since the term $(v_j - v_i)$ is zero when $j = i$. Therefore, the definition for β_{ij} in (2) is valid only for $j \neq i$. β_{ii} for $i \in [1, N]$ remains undefined at this point (we will later define it in order to simplify the analysis). To summarize the discussion above, we re-write the velocity equation in (1) as follows:

$$\begin{aligned}
\dot{v}_i &= \beta \sum_{j\in I_i} \beta_{ij} \left(v_j - v_i\right) + l_i = \beta \sum_{j=1}^{N} \beta_{ij} \left(v_j - v_i\right) + l_i && (7)\\
&= \beta \left(\sum_{j\in\Gamma_i} \beta_{ij}(v_j - v_i) + \sum_{j\in\Gamma_i'} \beta_{ij}(v_j - v_i) \right) + l_i \\
&= \beta \sum_{j\in\Gamma_i} \beta_{ij}(v_j - v_i) + l_i && (8)
\end{aligned}$$

There are two mechanisms by which β_{ij} may vanish: ζ_{ij} and $\phi(\|x_i - x_j\|)$ which represent, respectively, connection and strength. Therefore, terms in the sum in (8) may be zero if $\|x_i - x_j\| \geq \sigma$. This motivates the need to define what we will term a *connected N-convoy*.

Definition II.5 (Maximal Connected Distance)**.** *The maximal distance between connected agents is defined by $\delta(t) := \max_{i\in[1,N],j\in\Gamma_i} \|x_i(t) - x_j(t)\|$, where $x_i(t)$ is meant the position component of the solution to (1) through the initial data evaluated at time t.*

Definition II.6 (Connected N-Convoy)**.** *A connected N-convoy is an N-convoy where*

1) *The connectivity matrix G is a weakly connected directed graph, that is, the undirected underlying graph obtained by replacing all directed edges of the graph with undirected edges is a connected graph [11].*
2) *The maximal distance between connected agents at the initial time does not exceed the communication distance cut-off, σ. That is, $\delta(t_0) < \sigma$.*

Convoys can have leaders which are meant to guide the convoy along a particular trajectory. We define them as follows:

Definition II.7. *Agent i is said to be a **leader** of a connected N-convoy at time $t \geq t_0$ if $\Gamma_i = \emptyset$. Agent i is said to be a **follower** of a connected N-convoy at time $t \geq t_0$ if it is not a **leader** at time $t \geq t_0$. Define $L \coloneqq \{i \in [1, N] : \Gamma_i = \emptyset\}$ to be the set of leaders in the convoy.*

Fig. 3 depicts 6 different convoy primitives: (a) single-leader single follower, (b) single-leader, multi-follower, (c) multi-leader, single-follower, (d) single-leader, convoy chain, (e) multi-leader, multi-follower, (f) single-leader, fully-connected.

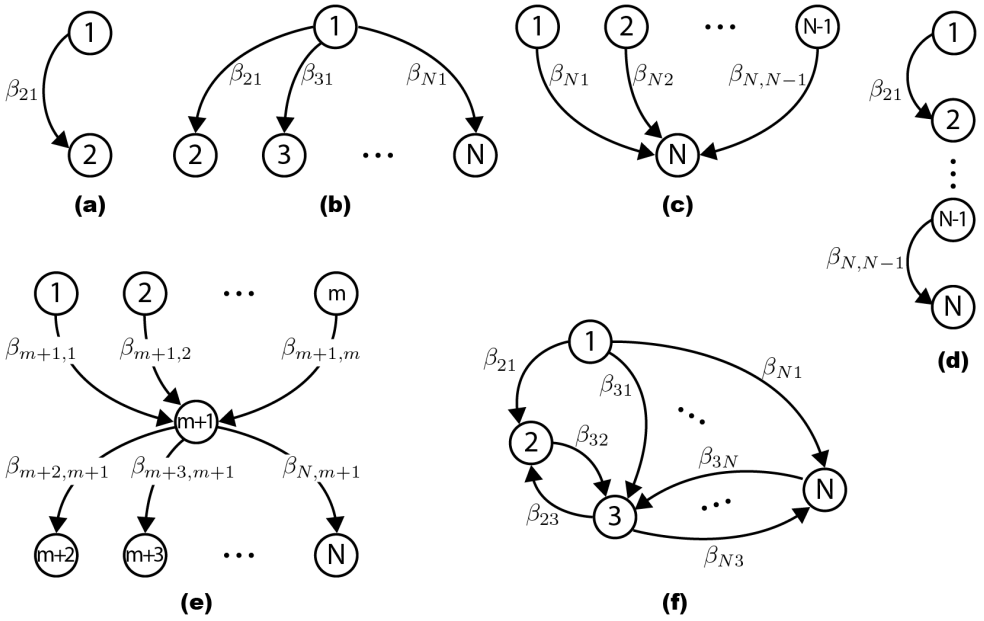

Fig. 3 6 different convoy primitives are illustrated: (a) single-leader single follower, (b) single-leader, multi-follower, (c) multi-leader, single-follower, (d) single-leader, convoy chain, (e) multi-leader, multi-follower, (f) single-leader, fully-connected.

We may normalize (1) as follows

$$\begin{cases} \dot{x}_i = v_i \\ \dot{v}_i = \alpha \sum\limits_{j \in \Gamma_i} a_{ij} \left(v_j - v_i\right) + l_i \\ x_i(t_0) = x_{i0}; v_i(t_0) = v_{i0} \end{cases} \tag{9}$$

where $a_{ij} = \frac{\beta_{ij}}{N}$ and $\alpha \coloneqq \beta N$. Define $a_{ii} = 1 - \sum_{j \in \Gamma_i} a_{ij},\ i \in [1, N]$. It follows that $\sum_{j=1}^{N} a_{ij} = 1$. We may lower bound a_{ii} as

$$\begin{aligned} a_{ii} &= 1 - \frac{1}{N} \sum_{j \in \Gamma_i} \phi(\|x_i - x_j\|) \geq 1 - \frac{N-1}{N} \\ &= \frac{1}{N} \geq \frac{\phi(\|x_u - x_v\|)}{N} \quad \forall\, u, v \in [1, N] \end{aligned} \tag{10}$$

The normalized system in (9) and lower bound in (10) will be used in the proof of Theorem II.1 stated below.

Finally, we define the term l_i.

$$l_i = \begin{cases} f_i(t) & \text{if } i \in L \\ \gamma_i \sum_{j \in \Gamma_i} r(\|x_i - x_j\|)(x_i - x_j) & \text{o/w} \end{cases} \tag{11}$$

where $\gamma_i \coloneqq \sqrt{\sum_{j \in \Gamma_i} \|v_i - v_j\|^2}$, $r : (0, \infty) \to [0, \infty)$ satisfies

1) For any $c \in (0, \sigma)$, we have $\int_0^c r(s)ds = \infty$
2) For any $c \in (0, \sigma)$, we have $\int_c^\infty r(s)ds < \infty$
3) $r(s) = 0$ for all $s \geq \sigma$

and f_i is a suitably smooth (exogenous) acceleration term such that the leader trajectory is bounded (a condition required in the theorem below). r represents a repulsive force whose strength increases as agents get close to one another. We assume that it too is limited by the sensing/communication distance (property 3 above). For brevity, we will often write $r_{ij} = r(\|x_i - x_j\|)$.

A. Sense and Follow Convoy Chain Architectures

Definition II.8. *A Sense and Follow Convoy Chain (SFCC) is a connected N-Convoy such that $|\Gamma_i| = 1$ for all $i \notin L$.*

It follows that an SFCC has the following properties:

1) There exists one and only one leader
2) Denote l to be the leader of the convoy. Then, for any $p \neq L$, there exists a unique path (connected collection of agents) from the leader to p. Denote this path by $\omega_p = \{n_1, n_2, \ldots, n_m\}$ where $n_i \in [1, N]$, $n_1 = l$, $n_m = p$, and $m \leq N$.

Loosely speaking, an SFCC can be any combination of primitive (b) and (d) in Fig. 3. The following theorem proves conditions under which an SFCC remains bounded.

Theorem II.1. *Consider an SFCC as stated in Definition II.8 and governed by (9). Suppose that the leader velocity, $v_l(t)$, is uniformly bounded and $\forall i \in [1, N]$ and $j \in \Gamma_i$ we have*

$$\|v_i(t_0) - v_j(t_0)\| < \alpha'_{i,j} \int_{\|x_i(t_0)-x_j(t_0)\|}^{\sigma} \phi^2(s)ds - \frac{1}{2} \int_{\|x_i(t_0)-x_j(t_0)\|}^{\sigma} r(s)ds \tag{12}$$

where $\alpha'_{i,j} = \alpha\lambda_{i,j}^2/N^2$. Then, the diameter of the convoy remains bounded, with bound given by

$$\sup_{t\in[t_0,\infty)} \max_{i,j\in[1,N]} \|x_i(t) - x_j(t)\| \leq (N-1)\sigma \tag{13}$$

and

$$\lim_{t\to\infty} \|v_i(t) - v_l(t)\| = 0 \tag{14}$$

for all $i \in [1, N]$.

The proof of Theorem II.1, including the definition of $\lambda_{i,j}$, is given in the appendix.

Corollary II.1. *Consider an SFCC that satisfies the conditions stated in Theorem II.1. Suppose, at time $t' > t_0$, a new agent k decides to follow a member i of the existing SFCC. If for all $j \in \Gamma_i \cup \{k\}$ we have*

$$\|v_i(t') - v_j(t')\| < \alpha'_{i,j} \int_{\|x_i(t')-x_j(t')\|}^{\sigma} \phi^2(s)ds - \frac{1}{2} \int_{\|x_i(t')-x_j(t')\|}^{\sigma} r(s)ds \tag{15}$$

Then, the new vehicle k may safely join in the sense of Theorem II.1.

Proof: Since we are guaranteed the original convoy remains connected at time t', we need only evaluate the impact of the new entrant, agent k on the velocity condition. If it holds, we apply Theorem II.1 to the new convoy. ■

Remark 3. *Corollary II.1 allows a service to check whether or not an agent can safely join an existing convoy. When a vehicle exits, however, a chain may break and additional conditions must be imposed on how the convoy should reconfigure. These scenarios will be addressed in a future paper.*

III. Unity Simulation Environment over the Web

In order to evaluate the performance of the convoy algorithms, we leveraged Unity, a cross-platform game engine developed by Unity Software Inc. We pursued a browser-based, client-server architecture where the unity project exported a webgl build that was loaded into a React front-end application served from the backend web-server. The approach is distributed in the sense that each vehicle or service agent executes locally. More specifically, each vehicle agent executes on a browser on a remote machine. By execute is meant the execution involving local CPU and memory to compute at each time step 6DOF rigid body vehicle dynamics, closed loop control, local convoy algorithms, and the rendering of the environment including other agents. Communication between agents is mediated via the web-sockets protocol. Specific data models encoding vehicle state were generated using the OPENAPI 3.0 specification. The architecture, shown in Fig. 4, enables any user with a NASA account to be able to access the server over an internal network and participate as a vehicle or service agent.

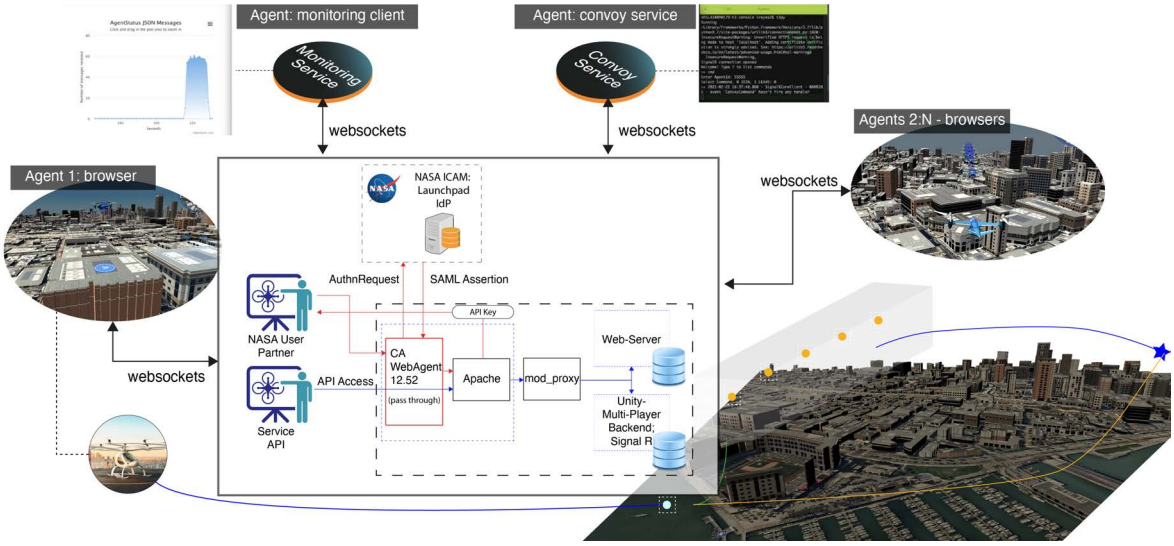

Fig. 4 The architecture of the simulation environment utilized an Apache front facing server together with a backend web-server and Unity multi-player backend. This also includes authentication and authorization using NASA Launchpad. API access is also available via an HMAC authentication approach.

IV. Simulation Examples

We now present two simulation examples that illustrate the proposed algorithm. The locally distributed convoy algorithms provide desired 4D waypoint information for each agent. The 4D waypoints must then be tracked by the vehicle's control system as depicted in Fig. 5. The UAM vehicle model utilized is similar to the one described in [12]. The control system employed is a nonlinear dynamic inversion control law. Details of both the model and control system are not included due to space limitations.

Example IV.1 (Joining a Convoy)**.** *In this example, we simulate (see Fig. 7) a convoy consisting of 7 vehicles and 1 leader. In ① (upper left) we show the matlab simulation (only two dimensions are displayed). Note that there is a coordinate transformation made between the matlab trajectory and that in Unity since Unity uses a left-handed coordinate system. In ② (upper right), we show the vehicle taking off from a building rooftop. In ③ (lower left), a pop-up message is displayed indicating that the cost to join the convoy is lower (better) than the cost to not join. In ④ (lower right), we show the vehicle joining the convoy and the other vehicles adjust their dynamics.*

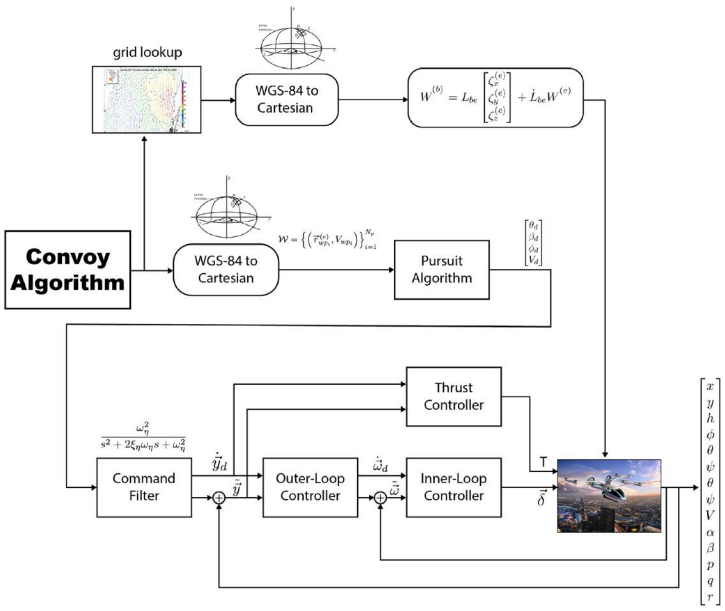

Fig. 5 Depicts how the output of the convoy algorithm is used to ultimately drive the agents' dynamics.

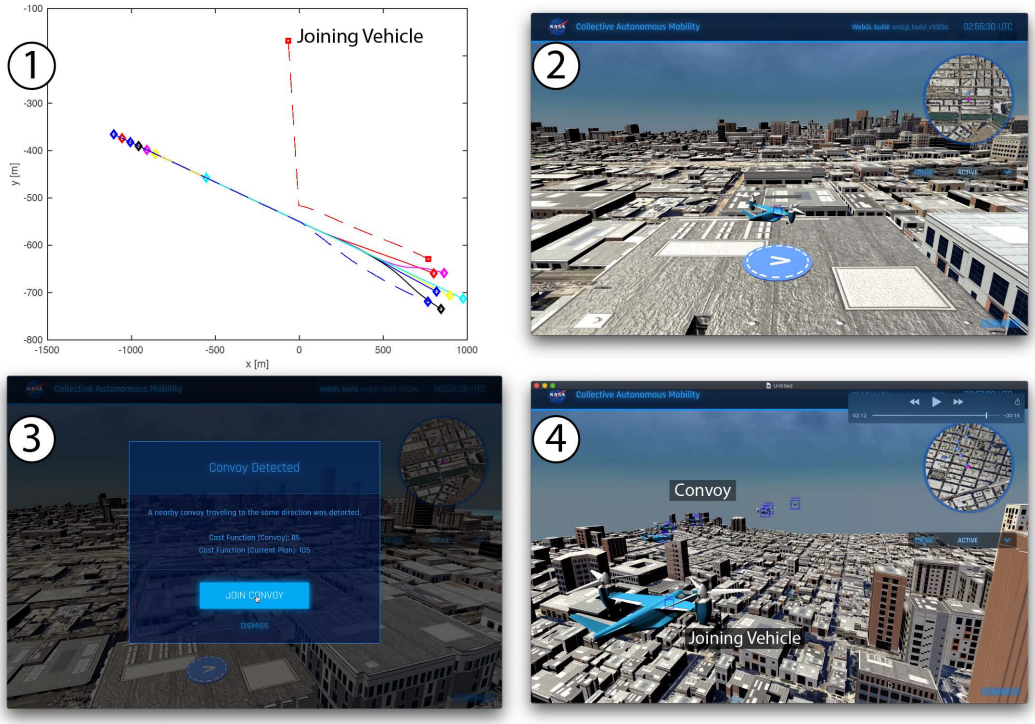

Fig. 6 Vehicle Joining a Convoy. In ① (upper left) we show the matlab simulation (only two dimensions are displayed). Note that there is a coordinate transformation made between the matlab trajectory and that in Unity since Unity uses a left-handed coordinate system. In ② (upper right), we show the vehicle taking off from a building rooftop. In ③ (lower left), a pop-up message is displayed indicating that the cost to join the convoy is lower (better) than the cost to not join. In ④ (lower right), we show the vehicle joining the convoy and the other vehicles adjust their dynamics.

Example IV.2 (Convoy Disturbance)**.** *In this example, we simulate a convoy intersecting with the trajectory of a balloon during taking off. Discussion of the balloon dynamics and control law used is beyond the scope of the current paper. In ① (upper left) we show the matlab simulation (only two dimensions are displayed). The balloon location is indicated in the figure and we observe the convoy moves around the balloon. Note that the leader does not move since it passes the balloon before the balloon takes off. In ② (upper right), we show the vehicle convoy approaching the location of the balloon. In ③ (lower left), we show the balloon taking off. In ④ (lower right), we show the vehicle convoy moving around the balloon as it ascends vertically.*

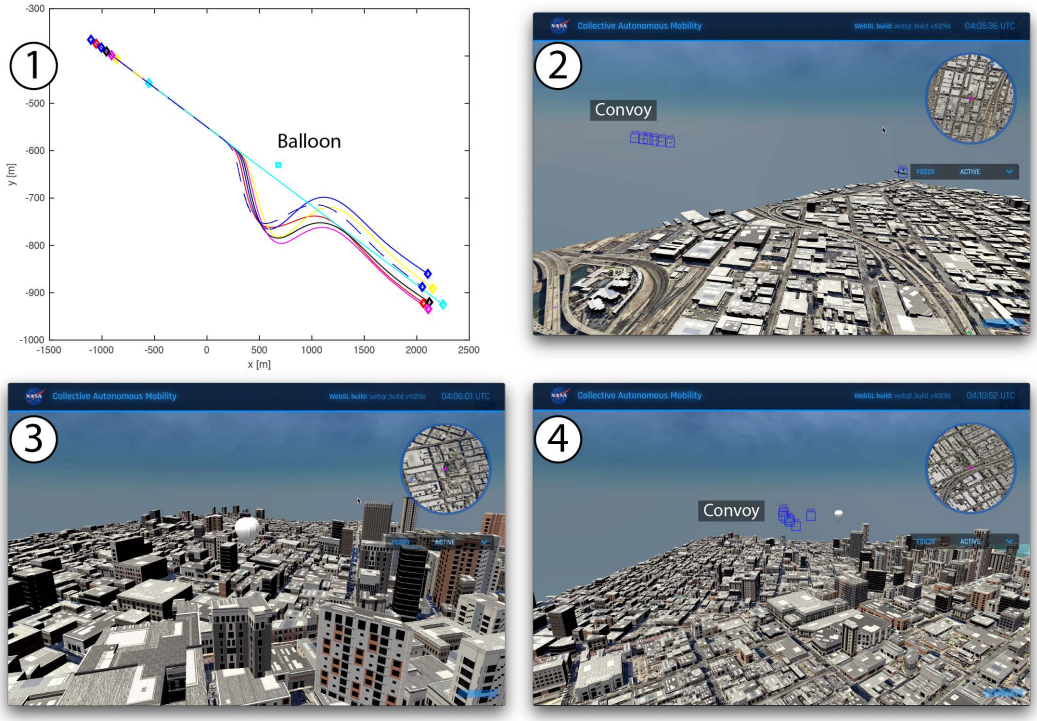

Fig. 7 Convoy Disturbance. In ① (upper left) we show the matlab simulation (only two dimensions are displayed). The balloon location is indicated in the figure and we observe the convoy moves around the balloon. Note that the leader does not move since it passes the balloon before the balloon takes off. In ② (upper right), we show the vehicle convoy approaching the location of the balloon. In ③ (lower left), we show the balloon taking off. In ④ (lower right), we show the vehicle convoy moving around the balloon as it ascends vertically.

V. Conclusions and Future Work

It is envisioned that over the next several decades, high density operations may become prevalent in the urban setting motivating the need for more efficient modes of operation. UAM vehicles grouped in autonomous convoys have the potential to lead to improved utilization of the airspace. This paper examined a class of convoy architectures and proved conditions under which the system remained bounded and velocity alignment occurred. To assess the convoy algorithms, we utilized a 6DOF rigid-body vehicle dynamics model for each agent. Unity, a cross-platform game engine, where 3-dimensional terrain, building, and vehicle data can be visualized was used to evaluate the system performance.

As systems move along their respective autonomy spectrums the need for locally distributed control algorithms that mitigate the shortcomings of human-centric, centralized ones is apparent. This approach, however, is not without its own set of unique challenges. Local interaction of agents executing (relatively) simple control laws can lead (in aggregate) to complex, emergent behavior that is difficult to predict in advance and whose stability and convergence properties are difficult to ascertain. There is a fundamental trade-off between systems exhibiting a high degree of emergence, often needed to improve system autonomy, and systems exhibiting a high degree of structure, often needed during the orderly landing at a vertiport, for example. Our future work aims to extend this research along these lines.

Appendix

A. Proof of Theorem II.1

We first state a lemma from [8] that will be needed in the following development.

Lemma V.1. *Let $S \in \mathbb{R}^{N\times N}$ denote a skew-symmetric matrix with $\max_{i,j}|S_{ij}| \le M$. Let u and w denote $\mathbb{R}^N$ vectors with non-negative entries. Let $\overline{U} = \sum_{j=1}^N u_j$, $\overline{W} = \sum_{j=1}^N w_j$, $\theta \in [0,\infty)$ and $\lambda(\theta) = |\Lambda(\theta)|$ where $\Lambda(\theta) = \{j : u_j \ge \theta\overline{U}$ and $w_j \ge \theta\overline{W}\}$. Then,*

$$| < Su, w > | \le M\overline{U}\overline{W}\left(1 - \lambda^2(\theta)\theta^2\right) \tag{16}$$

The next lemma bounds the norm of the derivative of the difference in positions between two agents.

Lemma V.2.

$$\frac{d}{dt}(\|x_i(t) - x_j(t)\|) \le \|v_i(t) - v_j(t)\| \tag{17}$$

Proof: Apply the chain rule to $\frac{d}{dt}(\|x_i(t) - x_j(t)\|^2)$ ■

The next lemma bounds the derivative of the difference in velocities between two agents.

Lemma V.3. *Let p, q be arbitrary with $p \ne q$. Then,*

$$(v_p - v_q)^T\left[\sum_{j=1}^N a_{pj}(v_j - v_p) - \sum_{k=1}^N a_{qk}(v_k - v_q)\right] \le \|v_p - v_q\|\left(d_{v_{pq}}\left(1 - \lambda_{pq}(\theta)\theta^2\right) - \|v_p - v_q\|\right) \tag{18}$$

where $d_{v_{pq}} := \max_{j\in\bar{\Gamma}_p, k\in\bar{\Gamma}_q}\|v_j - v_k\|, \lambda_{pq} = |\Lambda_{pq}|, \theta \in [0,\infty), \Lambda_{pq} = \left\{j : a_{pj} \ge \theta$ and $a_{qj} \ge \theta\right\}$

Proof: We have

$$\begin{aligned}
&(v_p - v_q)^T\left[\sum_{j=1}^N a_{pj}(v_j - v_p) - \sum_{k=1}^N a_{qk}(v_k - v_q)\right] \\
&= (v_p - v_q)^T\left[\sum_{j=1}^N\sum_{k=1}^N a_{pj}a_{qk}(v_j - v_k) - (v_p - v_q)\right] \\
&= \left[\sum_{j=1}^N\sum_{k=1}^N a_{pj}a_{qk}\langle v_p - v_q, v_j - v_k\rangle - \|v_p - v_q\|^2\right]
\end{aligned} \tag{19}$$

Consider the term: $\sum_{j=1}^N\sum_{k=1}^N a_{pj}a_{qk}\langle v_p - v_q, v_j - v_k\rangle = \langle S\bar{a}_q, \bar{a}_p\rangle$ where $S_{jk} := \langle v_p - v_q, v_j - v_k\rangle, \bar{a}_p = [a_{p1}\ a_{p2}\ \cdots\ \alpha_{pN}]^T$, and $\bar{a}_q = [a_{q1}\ a_{q2}\ \cdots\ \alpha_{qN}]^T$. Since $a_{pj} = 0$ for all $j \in \Gamma'_p$ and $a_{qj} = 0$ for all $j \in \Gamma'_q$, there exists a skew-symmetric matrix $\bar{S} \in \mathbb{R}^{N\times N}$ such that

$$\langle S\bar{a}_q, \bar{a}_p\rangle = \langle \bar{S}\bar{a}_q, \bar{a}_p\rangle \tag{20}$$

$$\max_{\substack{j\in[1,N]\\k\in[1,N]}}|\bar{S}_{jk}| = \max_{\substack{j\in\bar{\Gamma}_p\\k\in\bar{\Gamma}_q}}|\bar{S}_{jk}| \tag{21}$$

We also have $\max_{\substack{j\in\bar{\Gamma}_p\\k\in\bar{\Gamma}_q}}|\bar{S}_{jk}| = \max_{\substack{j\in\bar{\Gamma}_p\\k\in\bar{\Gamma}_q}}|\langle v_p - v_q, v_j - v_k\rangle| \le \|v_p - v_q\|\max_{\substack{j\in\bar{\Gamma}_p\\k\in\bar{\Gamma}_q}}\|v_j - v_k\|$. It follows using Lemma V.1 that

$$\begin{aligned}
\sum_{j=1}^N\sum_{k=1}^N a_{pj}a_{qk}\langle v_p - v_q, v_j - v_k\rangle &= \langle S\bar{a}_q, \bar{a}_p\rangle \\
&= \langle \bar{S}\bar{a}_q, \bar{a}_p\rangle \\
&\le M\bar{U}\bar{W}(1 - \lambda_{pq}^2(\theta)\theta^2)
\end{aligned} \tag{22}$$

where $M = \|v_p - v_q\| d_{v_{pq}}, \bar{U} = 1, \bar{W} = 1, \lambda_{pq} = |\Lambda_{pq}|, \theta \in [0, \infty)$, and $\Lambda_{pq} = \{j : a_{pj} \geq \theta \text{ and } a_{qj} \geq \theta\}$. Using the above bound in (19) completes the proof. ∎

We now prove Theorem II.1.

Proof: For any $p, q \in [1, N]$, we have

$$\begin{aligned} \|x_p(t) - x_q(t)\| &\leq \|x_p(t) - x_l(t)\| + \|x_l(t) - x_q(t)\| \\ \|v_p(t) - v_q(t)\| &\leq \|v_p(t) - v_l(t)\| + \|v_l(t) - v_q(t)\| \end{aligned} \tag{23}$$

We will show that the right hand side of (23) is suitably bounded leading us to conclude that there exists a $c_{pq} > 0$, independent of t such that $\sup_t \|x_p - x_q\| < c_{pq}$ and $\lim_{t\to\infty} \|v_p - v_q\| = 0$. Since p and q are arbitrary, we conclude the diameter of the convoy is bounded and the velocities converge to that of the leader.

Let $p \notin L$ be arbitrary. Consider the following statement:

$P(s)$: If

$$\|v_{n_s}(t_0) - v_{n_{s+1}}(t_0)\| < \alpha'_{n_s,n_{s+1}} \int_{\|x_{n_s}(t_0) - x_{n_{s+1}}(t_0)\|}^{\sigma} \phi^2(r)dr - \frac{1}{2} \int_{\|x_{n_s}(t_0) - x_{n_{s+1}}(t_0)\|}^{\sigma} r(s)ds \tag{24}$$

then,

1) there exists constants $b(s) \in (0, \sigma)$ and $c(s) \in (0, \sigma)$ with $c(s) < b(s)$ such that $c(s) \leq \|x_{n_s}(t) - x_{n_{s+1}}(t)\| \leq b(s)$ for all $t \geq t_0$
2) $\lim_{t\to\infty} \|v_{n_s}(t) - v_{s+1}(t)\| = 0$
3) $v_{n_s}(t)$ and $v_{n_{s+1}}(t)$ are uniformly bounded.

We prove via mathematical induction that $P(s)$ holds for any s along the path, that is, for any $s \in [1, m-1]$.

Base Case: $P(1)$: We compute

$$\begin{aligned} \frac{d}{dt}\|v_{n_1} - v_{n_2}\|^2 = 2(v_{n_1} - v_{n_2})^T \Bigg(\alpha \Bigg(\sum_{j\in\Gamma_{n_1}} a_{n_1,j}(v_j - v_i) - \sum_{k\in\Gamma_{n_2}} a_{n_2}(v_k - v_{n_2}) \Bigg) \\ + \gamma_{n_1} \sum_{j\in\Gamma_{n_1}} r_{n_1,j}(x_{n_1} - x_j) - \gamma_{n_2} \sum_{k\in\Gamma_{n_2}} r_{n_2,k}(x_{n_2} - x_k) \Bigg) \end{aligned} \tag{25}$$

Using Lemma V.3, with $\bar{\Gamma}_{n_1} = \{n_1\}$ and $\bar{\Gamma}_2 = \{n_1, n_2\}$, we have

$$\frac{d}{dt}\|v_{n_1} - v_{n_2}\|^2 \leq -2\alpha\lambda^2_{n_1,n_2}(\theta)\theta^2\|v_{n_1} - v_{n_2}\|^2 - 2\gamma_{n_2} r_{n_2,n_1}(v_{n_1} - v_{n_2})^T(x_{n_1} - x_{n_2}) \tag{26}$$

This implies (using the chain rule on the LHS of (26) and dividing by $2\gamma_{n_2} = 2\|v_{n_2} - v_{n_1}\|$)

$$\frac{d}{dt}\|v_{n_1} - v_{n_2}\| \leq -\alpha\lambda^2_{n_1,n_2}(\theta)\theta^2\|v_{n_1} - v_{n_2}\| - r_{n_2,n_1}(v_{n_1} - v_{n_2})^T(x_{n_1} - x_{n_2}) \tag{27}$$

Recall that $\Lambda_{n_1,n_2} = \{j : a_{n_1 j} \geq \theta \text{ and } a_{n_2 j} \geq \theta\} = \Lambda_{n_1} \cap \Lambda_{n_2}$. Consider the first set $\Lambda_{n_1}(\theta) = \{j : a_{n_1 j} \geq \theta\}$. Since $\bar{\Gamma}_{n_1} = \{n_1\}$, $\Lambda_{n_1}(\theta) = \{n_1\}$ if $\theta = \phi(\|x_{n_1} - x_{n_2}\|)/N$ (using (10)). Consider the second set $\Lambda_{n_2}(\theta) = \{j : a_{n_2 j} \geq \theta\}$. Since $\bar{\Gamma}_{n_2} = \{n_1, n_2\}$, $\Lambda_{n_2}(\theta) = \{n_1, n_2\}$ if $\theta = \phi(\|x_{n_1} - x_{n_2}\|)/N$ (again using (10)). Hence, $\Lambda_{n_1,n_2} = \{n_1\}$ if $\theta = \phi(\|x_{n_1} - x_{n_2}\|)/N$. It follows that $\lambda_{n_1,n_2} = 1$. The bound in (27) becomes:

$$\frac{d}{dt}\|v_{n_1} - v_{n_2}\| \leq -\alpha\frac{\phi^2(\|x_{n_1} - x_{n_2}\|)}{N^2}\|v_{n_1} - v_{n_2}\| - r_{n_2,n_1}(v_{n_1} - v_{n_2})^T(x_{n_1} - x_{n_2}) \tag{28}$$

Next, define $V(t) \coloneqq \|v_{n_1}(t) - v_{n_2}(t)\| + \frac{1}{2}\int_{\|x_{n_1}(t) - x_{n_2}(t)\|}^{\sigma} r(s)ds$. Computing the derivative of V along the solution to (9), we obtain (using (37))

$$\dot{V} \leq -\alpha\phi^2(\|v_{n_1} - v_{n_2}\|)/N^2\|v_{n_1} - v_{n_2}\| \tag{29}$$

(29) implies that $\dot{V} \leq 0$; hence, we may write

$$\|v_{n_1}(t) - v_{n_2}(t)\| + \frac{1}{2}\int_{\|x_{n_1}(t)-x_{n_2}(t)\|}^{\sigma} r(s)ds \leq V(t_0) \quad \forall t \geq t_0 \tag{30}$$

(30) implies that

$$\frac{1}{2}\int_{\|x_{n_1}(t)-x_{n_2}(t)\|}^{\sigma} r(s)ds \leq V(t_0) \quad \forall t \geq t_0 \tag{31}$$

(31) together with property 1 of $r(s)$ (listed below equation (11)) imply there exists a constant $c(1) > 0$ such that $\|x_{n_1}(t) - x_{n_2}(t)\| \geq c(1)\ \forall t \geq t_0$ which proves collision avoidance. We next integrate (29) to obtain

$$V(t) - V(t_0) \leq -\alpha'_{n_1,n_2}\int_{t_0}^{t} \phi^2(\|x_{n_1}(\tau) - x_{n_2}(\tau)\|)\|v_{n_1}(\tau) - v_{n_2}(\tau)\|d\tau \tag{32}$$

(32) implies that

$$\alpha'_{n_1,n_2}\int_{t_0}^{t} \phi^2(\|x_{n_1}(\tau) - x_{n_2}(\tau)\|)\|v_{n_1}(\tau) - v_{n_2}(\tau)\|d\tau \leq V(t_0) \tag{33}$$

Using Lemma V.2 and a change in variable ($\nu = \|x_{n_1}(\tau) - x_{n_2}(\tau)\|$) in (33), we obtain

$$\alpha'_{n_1,n_2}\int_{\|x_{n_1}(t_0)-x_{n_2}(t_0)\|}^{\|x_{n_1}(t)-x_{n_2}(t)\|} \phi^2(\nu)d\nu \leq \|v_{n_1}(t_0) - v_{n_2}(t_0)\| + \frac{1}{2}\int_{\|x_{n_1}(t_0)-x_{n_2}(t_0)\|}^{\sigma} r(s)ds \quad \forall t \geq t_0 \tag{34}$$

Let $t' \coloneqq \inf\{t \geq t_0 : \|x_{n_1}(t) - x_{n_2}(t)\| = \sigma\}$. We claim $t' = \infty$. Suppose this is not the case. Then, (34) yields

$$\alpha'_{n_1,n_2}\int_{\|x_{n_1}(t_0)-x_{n_2}(t_0)\|}^{\sigma} \phi^2(\nu)d\nu \leq \|v_{n_1}(t_0) - v_{n_2}(t_0)\| + \frac{1}{2}\int_{\|x_{n_1}(t_0)-x_{n_2}(t_0)\|}^{\sigma} r(s)ds \quad \forall t \geq t_0$$

This in in contradiction with (24). Therefore, we conclude that there exists a positive constant, $b(1) < \sigma$ such that

$$\|x_{n_1}(t) - x_{n_2}(t)\| \leq b(1) \quad \forall t \geq t_0 \tag{35}$$

Using (29), (35), and the fact that ϕ is non-increasing, we obtain $\dot{V} \leq -\alpha'_{n_1,n_2}\phi^2(b(1))\|v_{n_1} - v_{n_2}\|$. Using this together with Barbalat's lemma, we conclude that $\lim_{t\to\infty}\|v_{n_1}(t) - v_{n_2}(t)\| = 0$. Since $v_{n_1}(t) = v_l(t)$ is bounded (by assumption), so too is $v_{n_2}(t)$ establishing $P(1)$.

Inductive Step: Assume $P(s-1)$ holds for some $s \in [2, m-1]$. We prove this implies $P(s)$. Since $P(s-1)$ holds, we have (1) $\sup_t \|x_{n_{s-1}}(t) - x_{n_s}(t)\| < b(s-1)$, (2) $\lim_{t\to\infty}\|v_{n_{s-1}}(t) - v_{n_s}(t)\| = 0$, and (3) $v_{n_{s-1}}$ and v_{n_s} are uniformly bounded. The assumption in statement $P(s)$ reads:

$$\|v_{n_s}(t_0) - v_{n_{s+1}}(t_0)\| < \alpha'_{n_s,n_{s+1}}\int_{\|x_{n_s}(t_0)-x_{n_{s+1}}(t_0)\|}^{\sigma} \phi^2(r)dr - \frac{1}{2}\int_{\|x_{n_s}(t_0)-x_{n_{s+1}}(t_0)\|}^{\sigma} r(s)ds \tag{36}$$

Since v_{n_s} is bounded (from the conclusion of $P(s-1)$), we may regard it to be a leader for $v_{n_{s+1}}$ and take $\bar{\Gamma}_{n_s} = \{n_s\}$. $\bar{\Gamma}_{n_{s+1}} = \{n_s, n_{s+1}\}$. As before, we use Lemma V.3 to obtain

$$\frac{d}{dt}\|v_{n_s} - v_{n_{s+1}}\| \leq -\alpha\frac{\phi^2(\|x_{n_s} - x_{n_{s+1}}\|)}{N^2}\|v_{n_s} - v_{n_{s+1}}\| - r_{n_s,n_{s+1}}(v_{n_s} - v_{n_{s+1}})^T(x_{n_s} - x_{n_{s+1}}) \tag{37}$$

Defining the functional $V(t) \coloneqq \|v_{n_1}(t) - v_{n_2}(t)\| + \frac{1}{2}\int_{\|x_{n_1}(t)-x_{n_2}(t)\|}^{\sigma} r(s)ds$, and following the same steps as in the $P(1)$ case, we conclude that (1) there exists constants $b(s) \in (0, \sigma)$ and $c(s) \in (0, \sigma)$ with $c(s) < b(s)$ such that $c(s) \leq \|x_{n_s}(t) - x_{n_{s+1}}(t)\| \leq b(s)$ for all $t \geq t_0$, (2) $\lim_{t\to\infty}\|v_{n_s}(t) - v_{n_{s+1}}(t)\| = 0$, and (3) v_{n_s} and $v_{n_{s+1}}$ are uniformly bounded. Therefore, $P(s)$ holds for any $s \in [1, m-1]$.

Given agent p, we have, via the triangle inequality

$$\begin{aligned} \|x_p - x_l\| &\leq \|x_{n_1} - x_{n_2}\| + \|x_{n_2} - x_{n_3}\| + \cdots + \|x_{n_{m-1}} - x_{n_m}\| \\ \|v_p - v_l\| &\leq \|v_{n_1} - v_{n_2}\| + \|v_{n_2} - v_{n_3}\| + \cdots + \|v_{n_{m-1}} - v_{n_m}\| \end{aligned} \tag{38}$$

Apply $P(s)$ above to each segment of the path to obtain

$$\begin{aligned} &\lim_{t\to\infty} \|v_p(t) - v_l(t)\| = 0 \\ &\sup_{t\in[t_0,\infty)} \|x_p(t) - x_l(t)\| < \infty \end{aligned} \tag{39}$$

Pick a $q \notin L$ and $q \neq p$. Apply the same steps as above to conclude

$$\begin{aligned} &\lim_{t\to\infty} \|v_q(t) - v_l(t)\| = 0 \\ &\sup_{t\in[t_0,\infty)} \|x_q(t) - x_l(t)\| < \infty \end{aligned} \tag{40}$$

Using (39), (40), and (23) we conclude that the diameter of the convoy remains bounded and that the velocities of each agent converge to the leader velocity. ■

References

[1] "Are Flying Cars Preparing for Takeoff?" `https://www.morganstanley.com/ideas/autonomous-aircraft`, 2019. Accessed: 2021-03-01.

[2] Idris, H., and Shen, N., "Estimating airspace capacity based on risk mitigation metrics," *Tenth USA/Europe Air Traffic Management Research and Development Seminar (ATM2013), Chicago*, 2013.

[3] Henke, C., Frohleke, N., and Bocker, J., "Advanced convoy control strategy for autonomously driven railway vehicles," *2006 IEEE Intelligent Transportation Systems Conference*, IEEE, 2006, pp. 1388–1393.

[4] Henke, C., Tichy, M., Schneider, T., Böcker, J., and Schäfer, W., "Organization and control of autonomous railway convoys," *Proceedings of the 9th International Symposium on Advanced Vehicle Control, Kobe, Japan*, Vol. 2, Citeseer, 2008.

[5] Khan, M., Turgut, D., and Bölöni, L., "A study of collaborative influence mechanisms for highway convoy driving," *Proceedings of International Workshop on Agents in Traffic and Transportation (ATT08), in conjunction with the Seventh Joint Conference on Autonomous and Multi-Agent Systems (AAMAS 2008)*, Citeseer, 2008, pp. 46–53.

[6] Heinovski, J., and Dressler, F., "Platoon formation: Optimized car to platoon assignment strategies a d protocols," *2018 IEEE Vehicular Networking Conference (VNC)*, IEEE, 2018, pp. 1–8.

[7] Cucker, F., and Smale, S., "Emergent behavior in flocks," *IEEE Transactions on automatic control*, Vol. 52, No. 5, 2007, pp. 852–862.

[8] Motsch, S., and Tadmor, E., "A new model for self-organized dynamics and its flocking behavior," *Journal of Statistical Physics*, Vol. 144, No. 5, 2011, pp. 923–947.

[9] Ha, S.-Y., Liu, J.-G., et al., "A simple proof of the Cucker-Smale flocking dynamics and mean-field limit," *Communications in Mathematical Sciences*, Vol. 7, No. 2, 2009, pp. 297–325.

[10] Cucker, F., and Dong, J.-G., "Avoiding collisions in flocks," *IEEE Transactions on Automatic Control*, Vol. 55, No. 5, 2010, pp. 1238–1243.

[11] "Connected Graph," `https://mathworld.wolfram.com/ConnectedGraph.html`, 2019. Accessed: 2021-03-01.

[12] Lombaerts, T., Kaneshige, J., Schuet, S., Aponso, B. L., Shish, K. H., and Hardy, G., "Dynamic Inversion based Full Envelope Flight Control for an eVTOL Vehicle using a Unified Framework," *AIAA Scitech 2020 Forum*, 2020, p. 1619.